

Supplementary Data

Identifying and applying a highly selective probe to simultaneously determine the *O*-glucuronidation activity of human UGT1A3 and UGT1A4

Li Jiang,^{1,+} Si-Cheng Liang,^{2,3,+} Chao Wang,¹ Guang-Bo Ge,² Xiao-Kui Huo,¹ Xiao-Yi Qi,⁴ Sa Deng,¹ Ke-Xin Liu¹ and Xiao-Chi Ma^{1,*}

¹ College of Pharmacy, Key Laboratory of Pharmacokinetic and Drug Transport of Liaoning, Academy of Integrative Medicine, Dalian Medical University, Dalian, 116044, China.

² Laboratory of Pharmaceutical Resource Discovery, Dalian Institute of Chemical Physics, Chinese Academy of Sciences, Dalian, China.

³ Graduate School of Chinese Academy of Sciences, Beijing, China.

⁴ Second Affiliated Hospital of Dalian Medical University, Dalian, China

Correspondence and requests for materials should be addressed to X.C. Ma (E-mail: maxc1978@163.com)

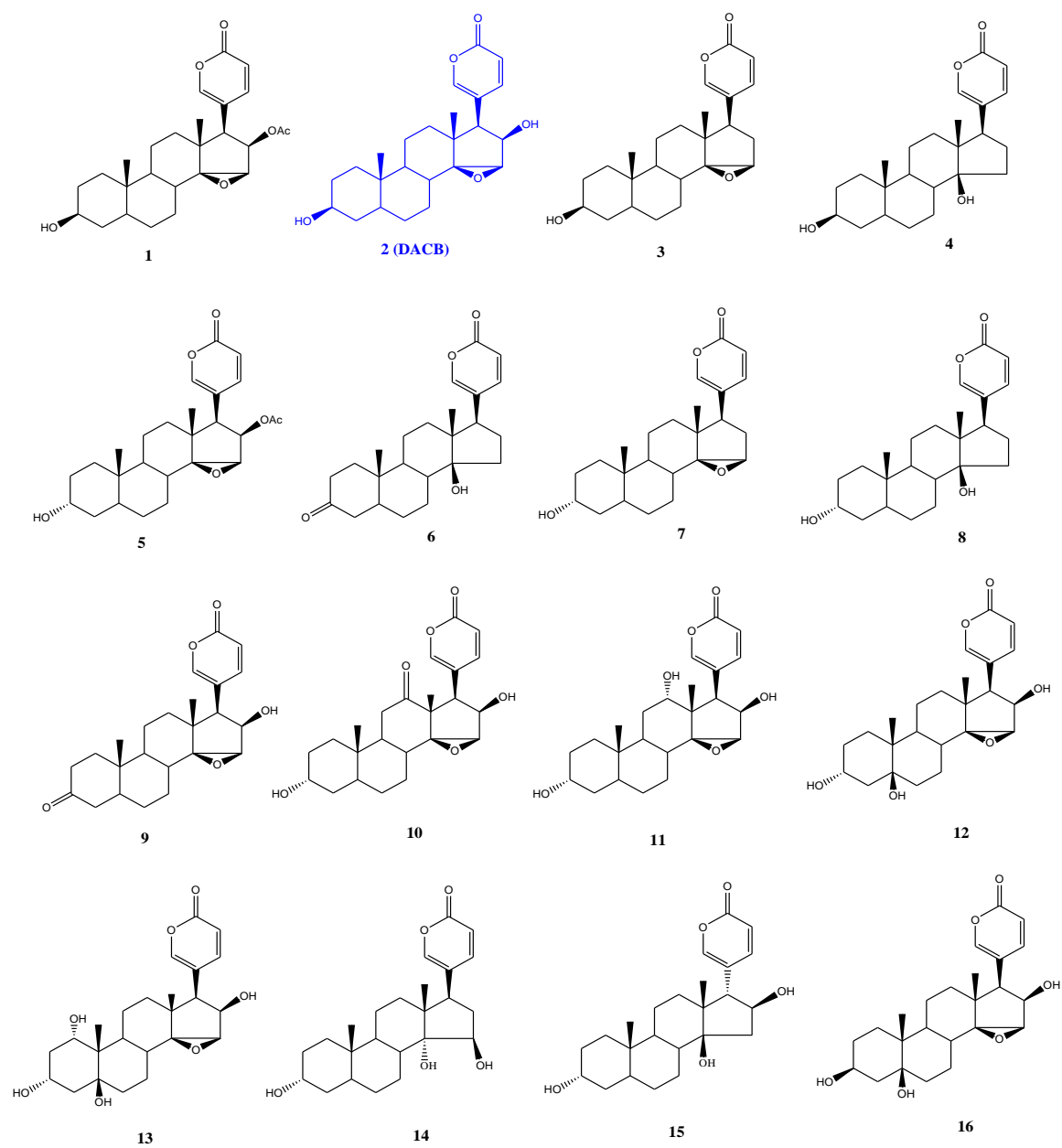
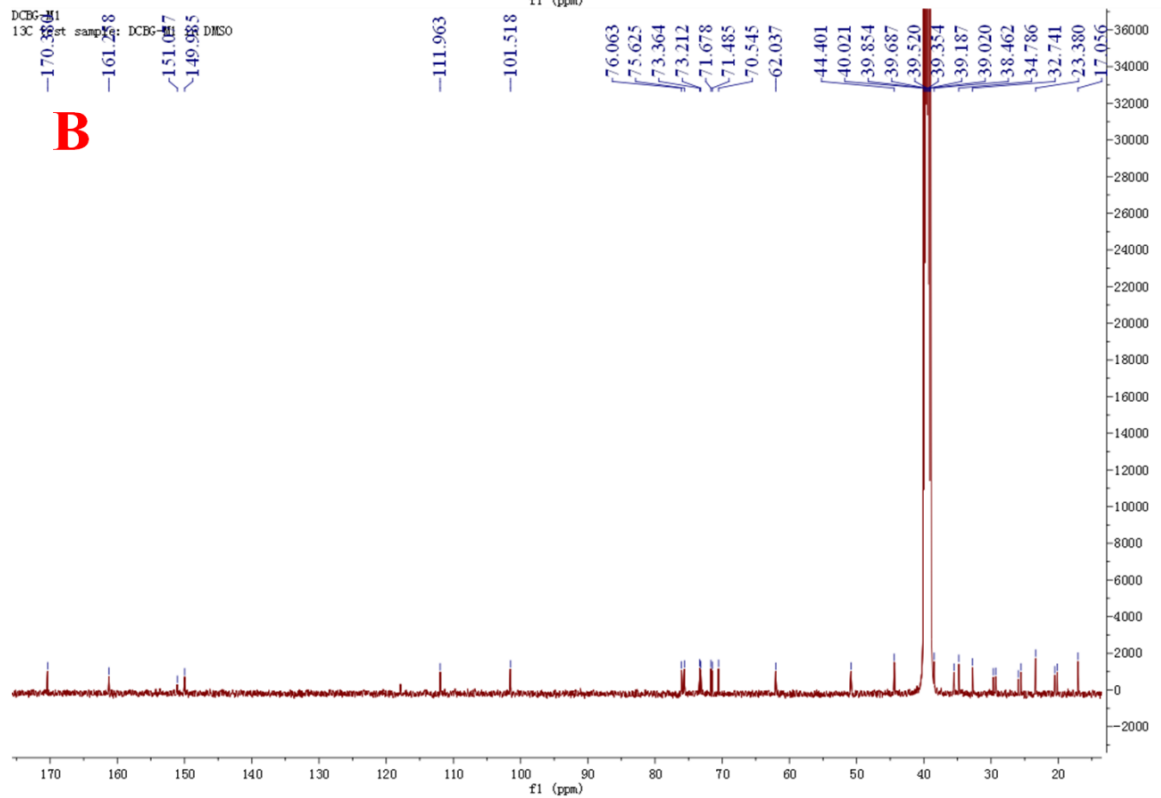
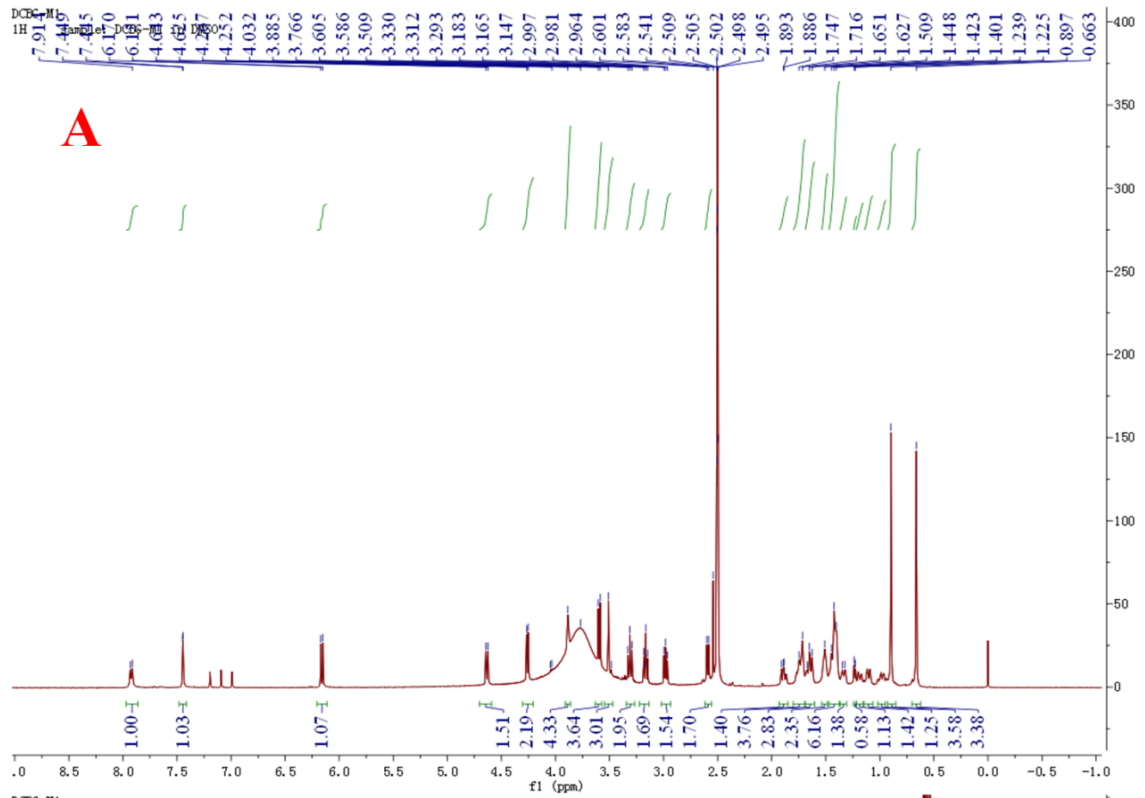


Fig. S1 Chemical structures of bufadienolides (1-16) used in the present work



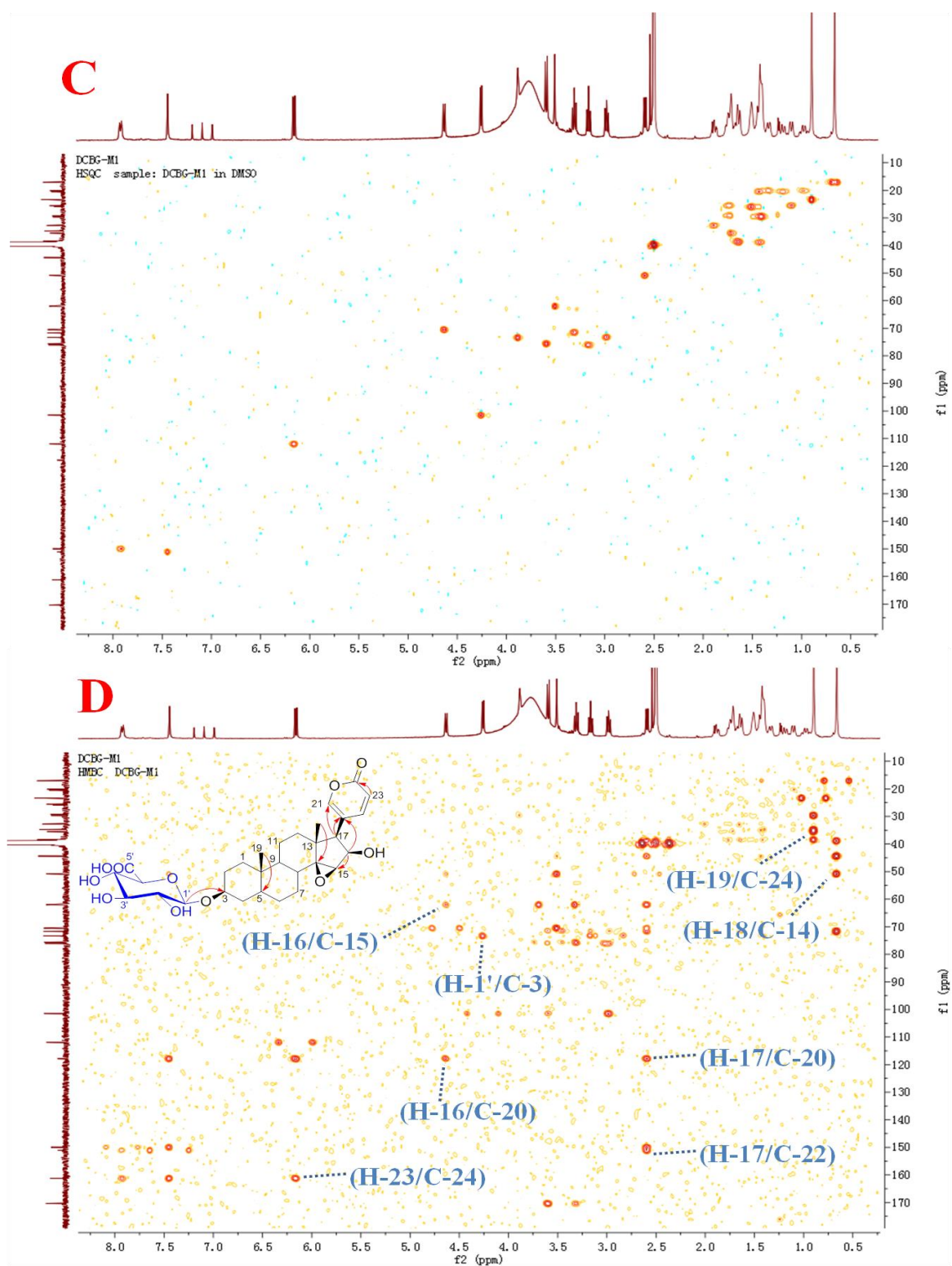
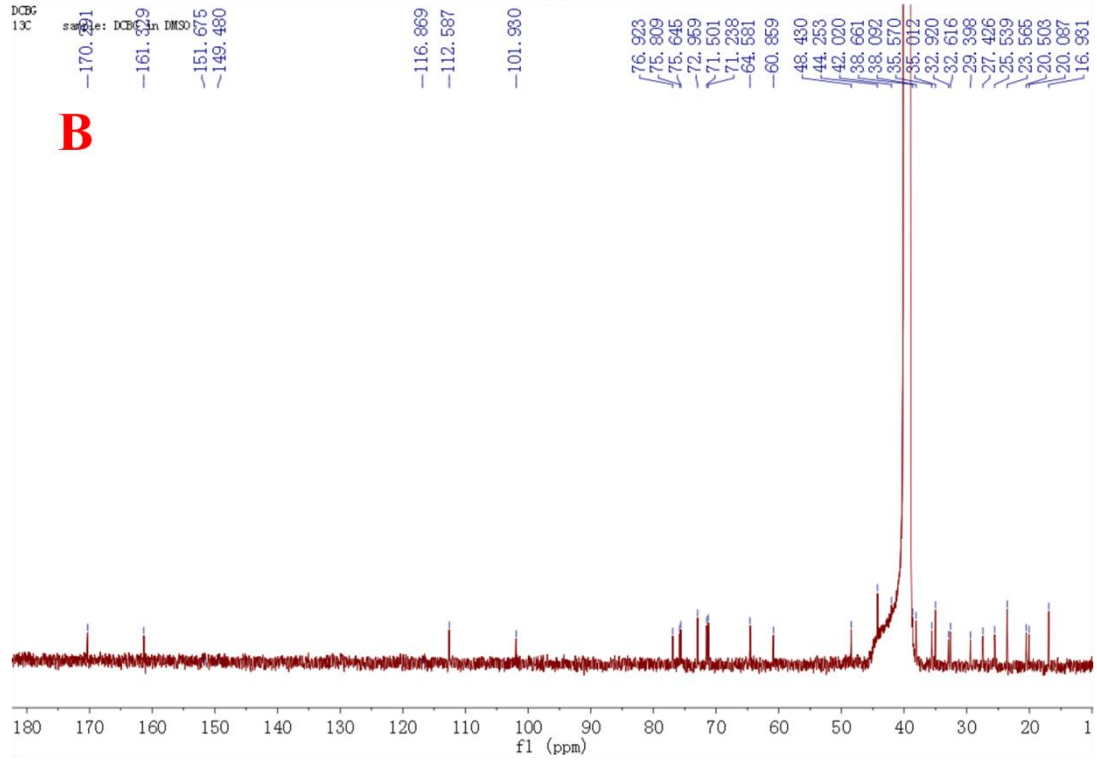
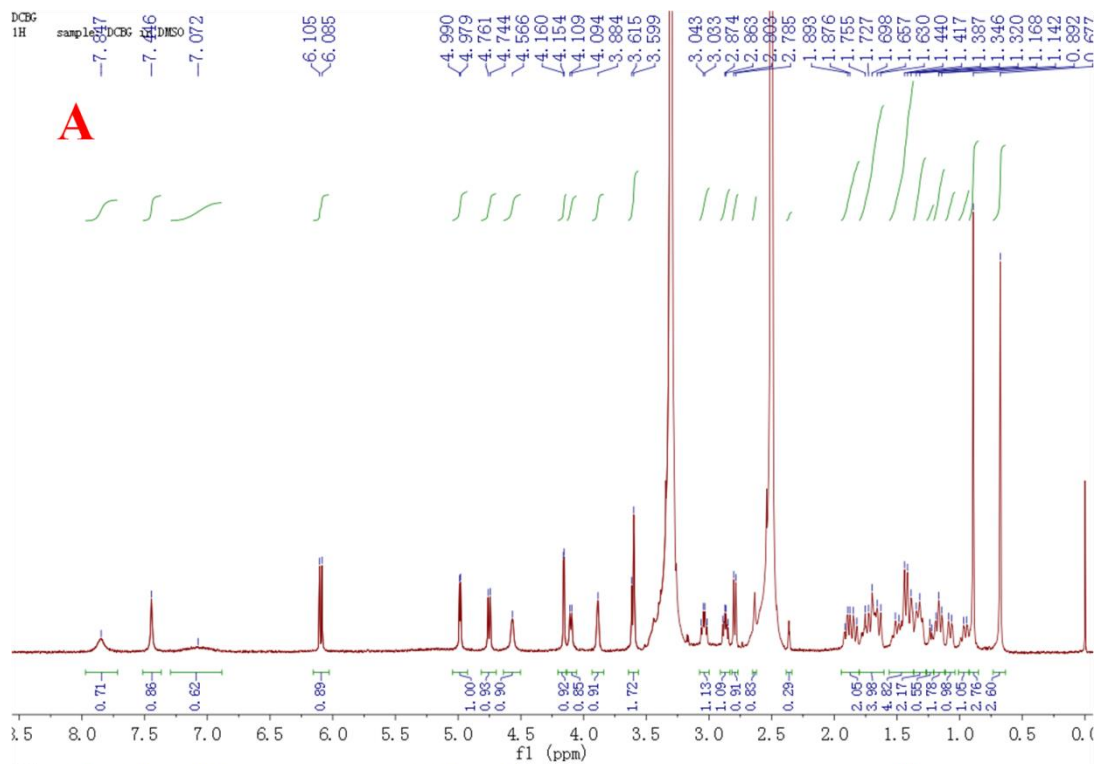


Fig. S2. The spectral data of M-1 (500MHz, DMSO). ^1H -NMR (A); ^{13}C -NMR (B); HMQC (C) and HMBC (D).



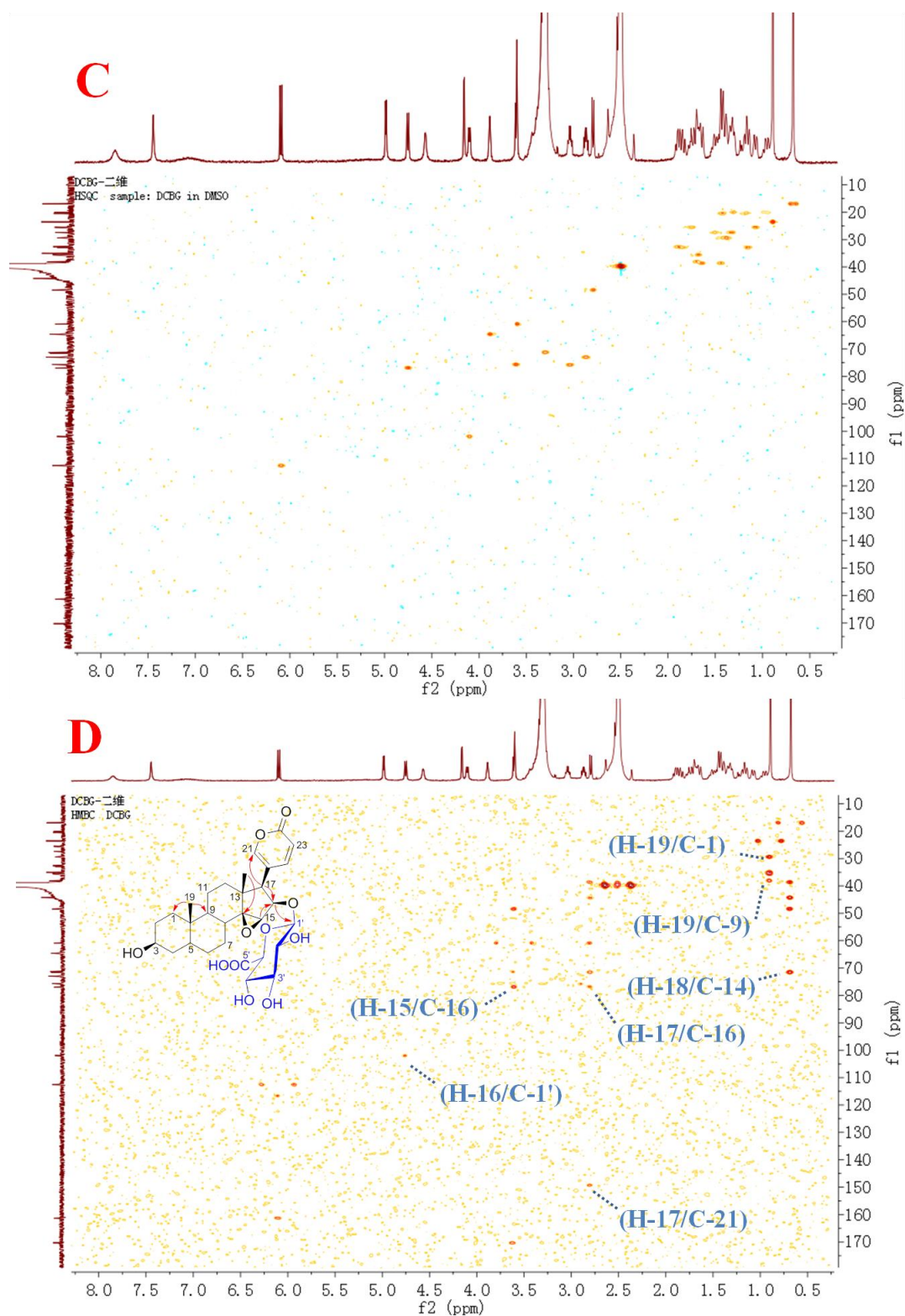


Fig. S3. The spectral data of M-2 (500MHz, DMSO). ¹H-NMR (A); ¹³C-NMR (B); HMQC (C) and HMBC (D).

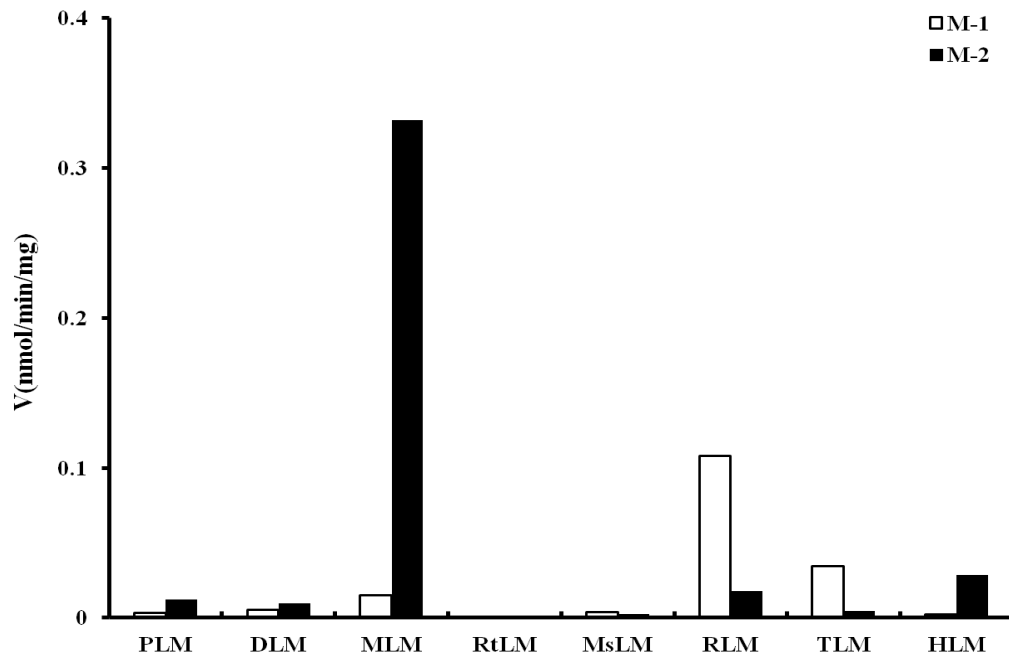


Fig. S4 The formation rates of M-1 and M-2 in various species, including PLMs, DLMs, MLMs, RtLMs, MsLMs, RLMs, TLMs and HLMs.

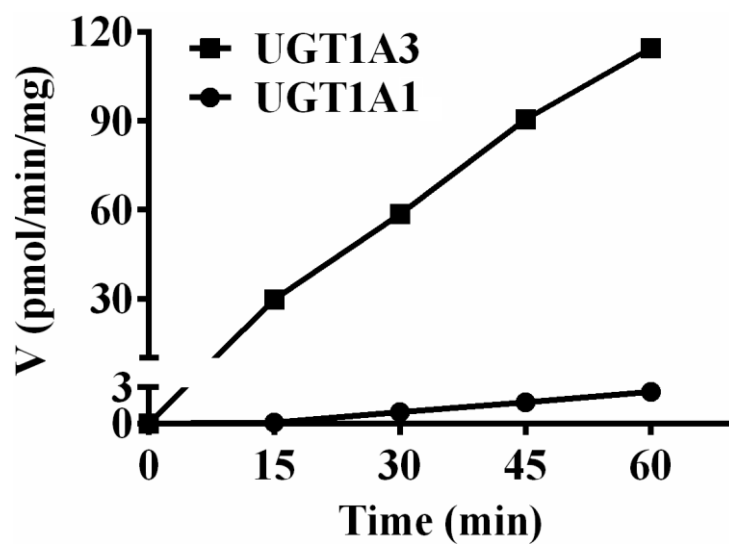


Fig. S5 Time courses for DACB-16-*O*-glucuronidation by UGT1A3 and UGT1A1. The final substrate concentration was 50 μ M. Each data point represents the mean of triplicate determinations.

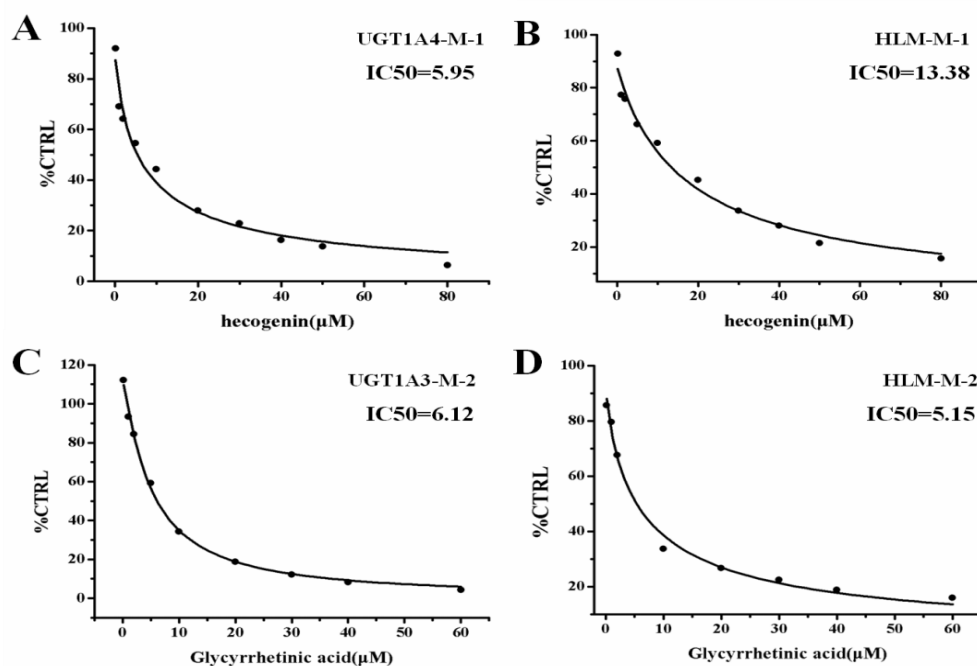


Fig. S6. IC₅₀ values of M-1 formation by hecogenin (a UGT1A4-specific inhibitor) in UGT1A4 samples (A) and HLMs (B); and IC₅₀ values for M-2 formation by glycyrrhethinic acid (a UGT1A3-specific inhibitor) in UGT1A3 samples (C) and HLMs (D), respectively.

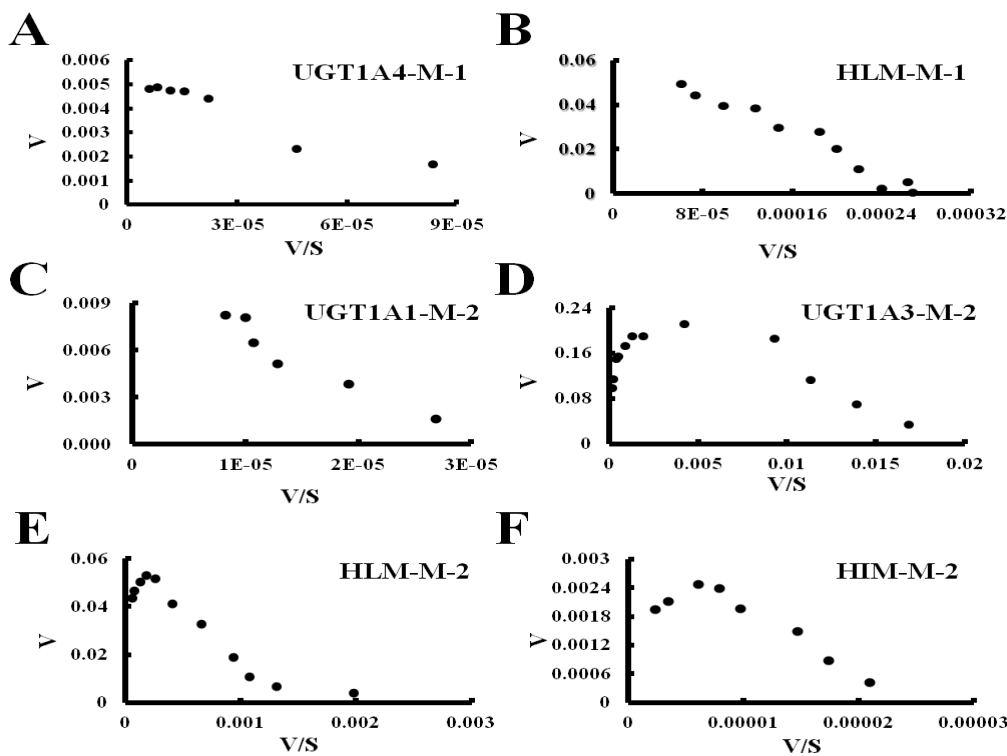


Fig. S7 Eadie-Hofstee plots of the glucuronidation profiles to determine the best-fit equation. (A) UGT1A4 samples for M-1; (B) HLMs for M-1; (C) UGT1A1 samples for M-2; (D) UGT1A3 samples for M-2; (E) HLMs for M-2; and (F) HIMs for M-2.

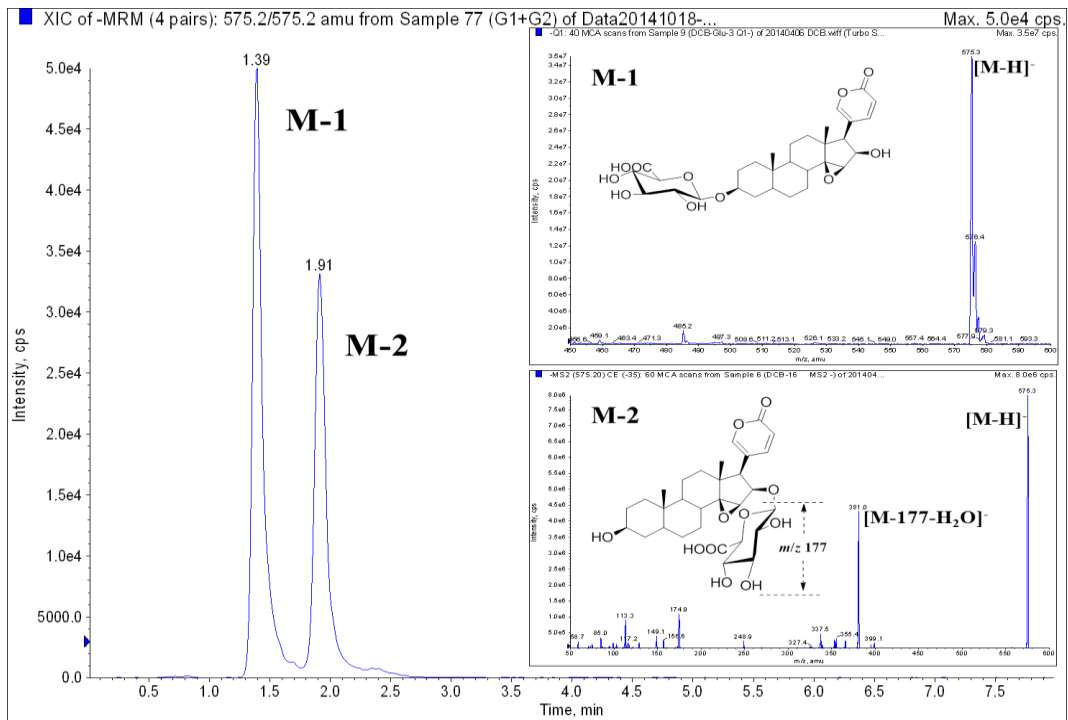


Fig. S8 MRM chromatogram of M-1 and M-2 in HLMs.

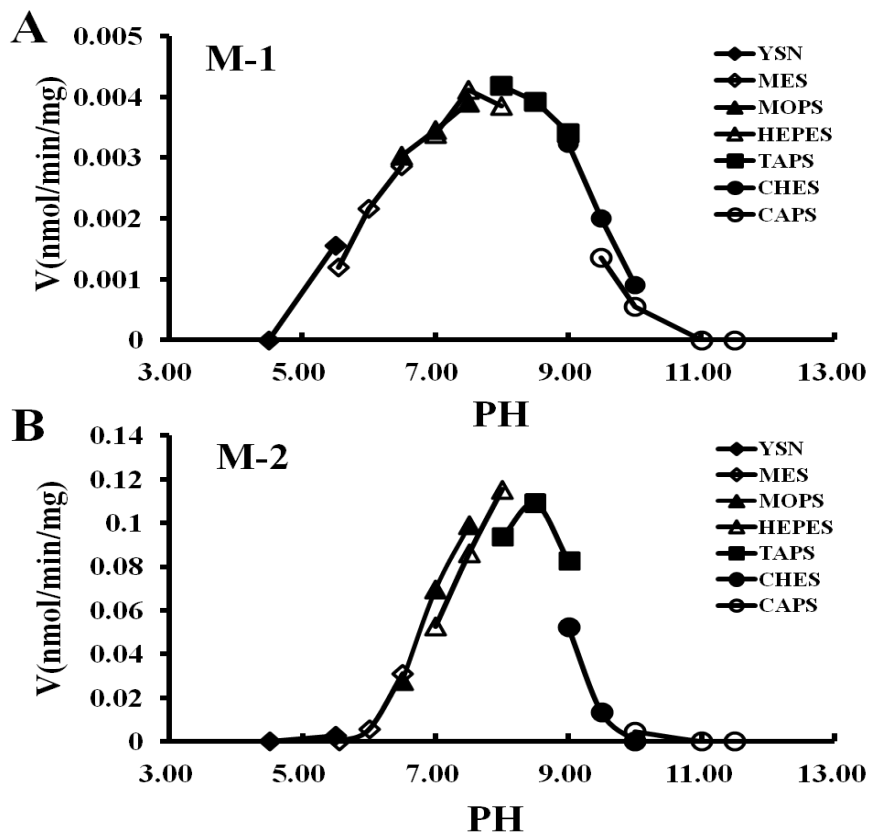


Fig. S9 The influences of various pH values for forming M-1(A) and M-2 (B).

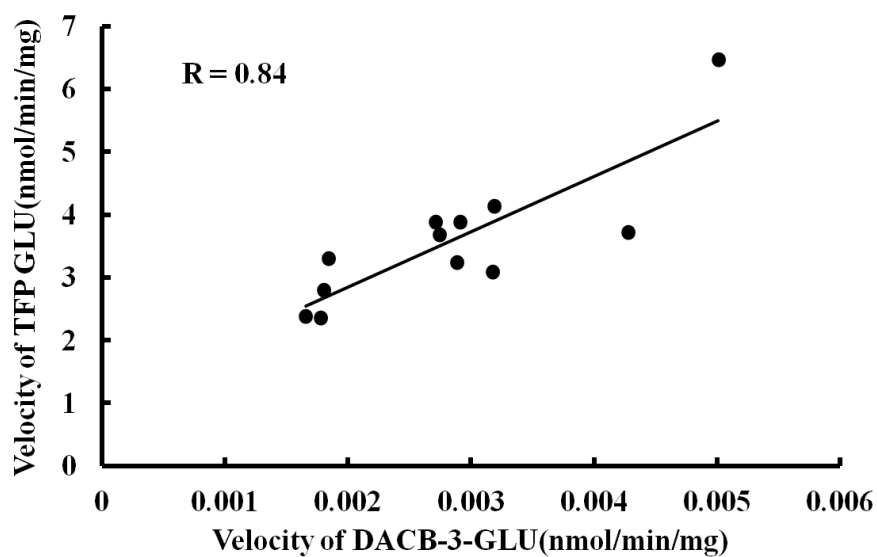


Fig. S10 The correlation analysis between DACB-3-*O*-glucuronidation rates by UGT1A4 and TFP-*N*-glucuronidation by UGT1A4 in 12 individual HLMs.

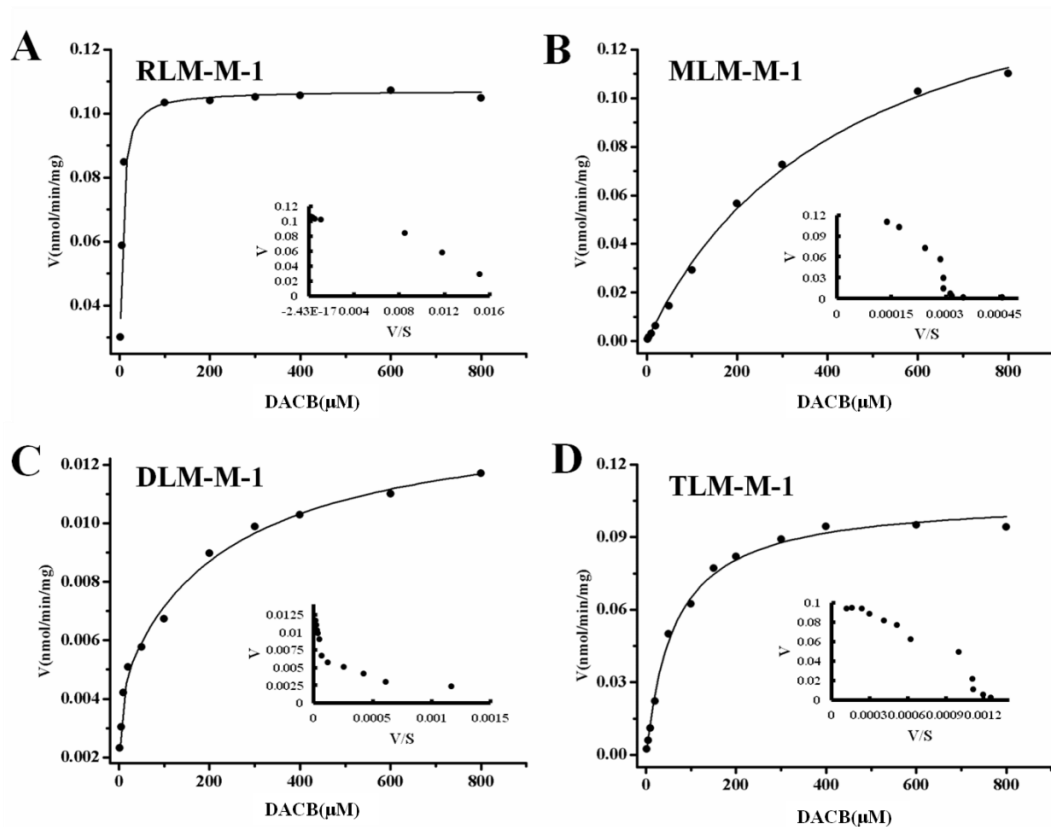


Fig. S11 The enzyme kinetics of DACB glucuronidation at C-3 (M-1) in animal liver microsomes. (A) Rabbit liver microsomes; (B) Monkey liver microsomes; (C) Dog liver microsomes and (D) Guinea pig liver microsomes.

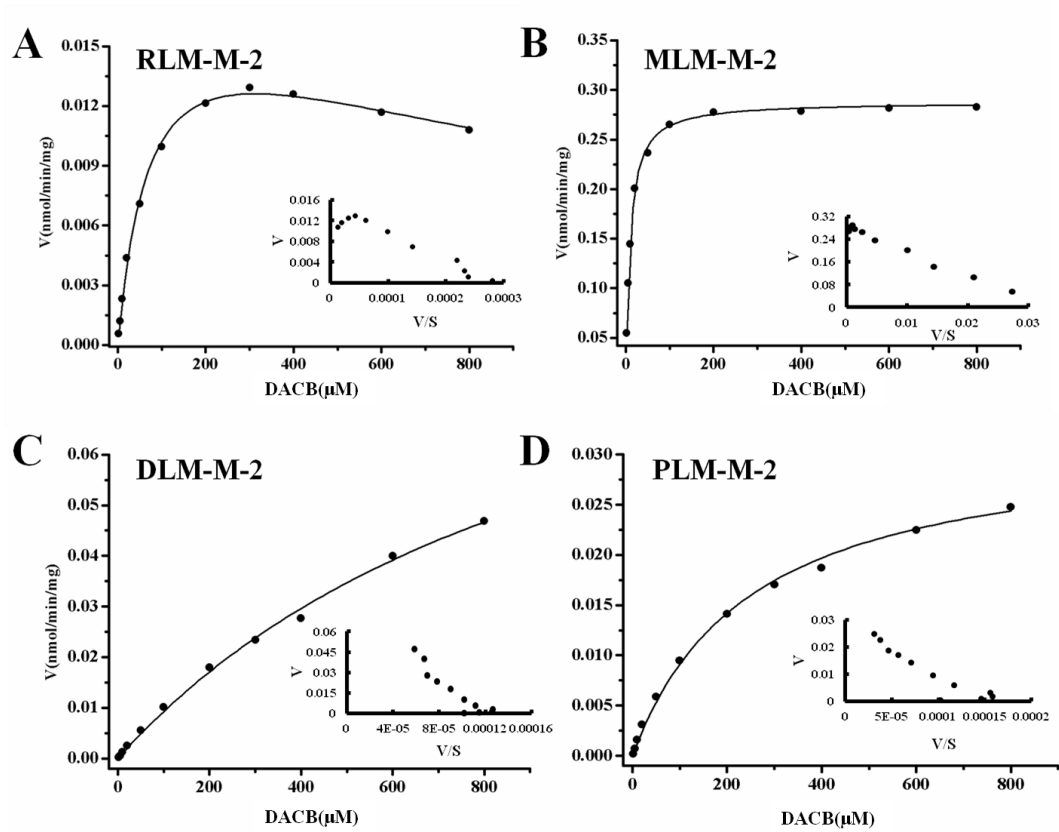


Fig. S12 The enzyme kinetics of DACB glucuronidation at C-16 (M-2) in animal liver microsomes. (A) Rabbit liver microsomes; (B) Monkey liver microsomes; (C) Dog liver microsomes and (D) Pig liver microsomes.

Table S1 ^1H - and ^{13}C NMR spectral data of M-1 and M-2 (DMSO- d_6)

No.	M-1		M-2	
	δ_{H} (500 MHz)	δ_{C} (125 MHz)	δ_{H} (500 MHz)	δ_{C} (125 MHz)
1	1.72 m	29.3	1.43 m	29.4
	1.41 m		1.38 m	
2	1.51 m	25.9	1.50 m	27.4
	1.44 m		1.32 m	
3	3.89 brs	73.4	3.88 s	64.6
4	1.50 m	29.7	1.84 m	32.6
	1.41 m		1.15 m	
5	1.72 m	35.5	1.70 m	35.6
6	1.74 m	25.5	1.75 m	25.5
	1.11 m		1.07 m	
7	1.44 m	20.5	1.43 m	20.5
	1.19 m		1.17 m	
8	1.89 m	32.7	1.87 m	32.9
9	1.65 m	38.5	1.70 m	38.1
10	—	34.8	—	35.0
11	1.34 m	20.2	1.31 m	20.1
	0.98 m		0.95 m	
12	1.65 m	38.7	1.64 m	38.7
	1.43 m		1.44 m	
13	—	44.4	—	44.3
14	—	71.7	—	71.5
15	3.51 brs	62.0	3.60 s	60.9
16	4.63 d (9.0)	70.5	4.79 brd (8.5)	76.9
17	2.59 d (9.0)	50.9	2.79 d (8.5)	48.4
18	0.66 s	17.1	0.68 s	16.9
19	0.90 s	23.4	0.89 s	23.6
20	—	117.9	—	116.6
21	7.45 d (2.0)	151.1	7.40 s	151.8
22	7.92 d (9.5)	150.0	7.80 brs	149.6
23	6.10 d (9.5)	112.0	6.10 d (10.0)	112.6
24	—	161.3	—	161.3
1'	4.26 d (7.5)	101.5	4.10 d (7.5)	101.9
2'	3.31 t (9.0)	71.5	3.30 m	71.2
3'	3.17 t (9.0)	76.1	3.04 m	75.9
4'	2.98 t (9.0)	73.2	2.87 m	73.0
5'	3.60 d (9.0)	75.6	3.61 d (8.0)	75.6
6'	—	170.4	—	170.3

Table S2 Kinetic parameters of DACB-*O*-glucuronidation in microsomes of experimental animals

Metabolites	Enzymes	K_m	V_{max}	Cl_{int}	K_i
		μM	nmol/min/mg	$\mu L/min/mg$	μM
3-<i>O</i>-Glucuronide (M-1)	RLMs	3.95 \pm 0.41	0.107 \pm 0.002	27.848	N/A
	MLMs	439.53 \pm 40.19	0.174 \pm 0.008	0.387	N/A
	DLMs	2.19 \pm 0.76	0.005 \pm 0.001	2.054	N/A
		241.13 \pm 63.40	0.009 \pm 0.001	0.038	N/A
	TLMs	63.58 \pm 5.33	0.106 \pm 0.002	1.730	N/A
16-<i>O</i>-Glucuronide (M-2)	RLMs	75.43 \pm 7.01	0.018 \pm 0.001	0.239	1284.5 \pm 187.2
	MLMs	9.18 \pm 0.41	0.288 \pm 0.002	31.59	N/A
	DLMs	1094.8 \pm 140.1	0.111 \pm 0.010	0.100	N/A
	PLMs	251.6 \pm 22.7	0.032 \pm 0.001	0.127	N/A